Selectivity enhancement of p-type semiconducting hydrocarbon sensors - the use of sol-precipitated nano-powders

Sahner, K.; Schönauer, D.; Matam, M.; Post, M.; Moos, R.

Publisher's version / Version de l'éditeur:
http://dx.doi.org/10.1016/j.snb.2007.09.024
Sensors and Actuators B: Chemical, 130, 1, pp. 470-476, 2008-03-14

Available online at www.sciencedirect.com
ScienceDirect
Sensors and Actuators B 130 (2008) 470–476
SENSORS AND ACTUATORS B CHEMICAL
www.elsevier.com/locate/snb

Selectivity enhancement of p-type semiconducting hydrocarbon sensors—The use of sol-precipitated nano-powders

K. Sahner [a,*], D. Schönauer [a], M. Matam [b], M. Post [b], R. Moos [a]

[a] *Functional Materials, University of Bayreuth, 95447 Bayreuth, Germany*
[b] *Institute for Chemical Process and Environmental Technology, National Research Council of Canada, Ottawa, Ontario K1A 0R6, Canada*

Available online 16 September 2007

Abstract

A method for preparing sol-precipitated $Sr(Ti_{0.8}Fe_{0.2})O_{3-\delta}$ powders yielding particle sizes of about 70 nm is presented. Screen-printed films based on such nano-scaled powders are compared and contrasted to conventional micro-scaled thick films.

By employing sol-precipitated powders, the hydrocarbon sensitivity of the sensor devices is improved. For unsaturated hydrocarbons, resistance changes similar to those of thin films prepared by pulsed laser deposition are observed, thus combining the fast sensor response of $Sr(Ti_{0.8}Fe_{0.2})O_{3-\delta}$ thick films with the high response (R/R_0) values observed for thin films. The pronounced cross-interference of NO and CO can be eliminated by means of an additional zeolite layer deposited on top of the nano-scaled sensor film.

Keywords: Sol precipitation; Zeolite; Pulsed laser deposition; Hydrocarbon sensor; $Sr(Ti_{0.8}Fe_{0.2})O_{3-\delta}$

1. Introduction

More stringent environmental regulations all over the world have increased the demand for inexpensive, accurate and reliable gas sensor devices. There are many examples of toxic or explosive gases that should be monitored, and these include CO, nitrous oxides, ammonia, hydrocarbons, hydrogen, etc. [1–3].

For cars equipped with a three-way catalyst, the need for a reliable "On-Board Diagnosis" (OBD) of the exhaust gas aftertreatment system might enforce an additional sensor downstream of the catalyst. To date, the catalyst functionality is monitored indirectly by correlating the oxygen storage capacity with the conversion efficiency. A decrease in the conversion rate and oxygen storage capacity of the catalyst results in an increase in the amplitudes of the λ-oscillations downstream from the three-way catalyst. The ratio of the amplitudes of λ-probes located upstream and downstream from the catalyst is thus a measure that can be used to evaluate catalyst efficiency [3]. In the future, however, a more direct and accurate method will be needed to determine whether or not the exhaust aftertreatment system of cars with lowest emissions meets the emission requirements. Therefore, a direct measurement method employing a sensor that detects the amount of unburnt hydrocarbons is desirable [4]. A hydrocarbon sensor can also be used for On-Board Diagnosis of close-coupled oxidation catalysts in diesel engines [5], or for safety applications, e.g. in Japan, where most of the households are equipped with propane-based heating systems.

Although n-type conducting metal oxides like SnO_2 or ZnO dominate the research effort in this sensor area, some p-type conducting ceramics have recently received more attention as well. These exceptions include the commercially available ammonia gas sensors, $Cr_{2-x}Ti_xO_3$ [6,7] and NO_x sensors based on perovskite rare-earth metal oxides of the $LnFeO_3$ family, where Ln is La, Nd, Sm, Gd and Dy [8].

The perovskite family $SrTi_{1-x}Fe_xO_{3-\delta}$ with $x = 0.1$–0.5 are promising materials for hydrocarbon sensing in the temperature range from 350 to 450 °C. With screen-printed films of about 20 μm thickness, a fast, stable and reversible response to hydrocarbons is observed. In particular, the $SrTi_{1-x}Fe_xO_{3-\delta}$ members with a moderate iron content ($x = 0.1$–0.2) show best performance [9,10].

The present work addresses selectivity enhancement of $SrTi_{0.8}Fe_{0.2}O_{3-\delta}$ based sensors. Whereas an earlier paper focused on an extrinsic method using an additional zeolite

* Corresponding author at: Functional Materials, University of Bayreuth, Universitätsstr. 30, D-95447 Bayreuth, Germany. Tel.: +49 921 55 7400; fax: +49 921 55 7405.
E-mail address: Functional.Materials@uni-bayreuth.de (K. Sahner).

0925-4005/$ – see front matter © 2007 Elsevier B.V. All rights reserved.
doi:10.1016/j.snb.2007.09.024

filter layer [11], the present contribution takes a closer look at the precursor material itself. As the sensor effect towards reducing gases includes a mechanism which is attributed to surface processes, i.e., a redox reaction taking place at the semiconductor surface, the sensitivity of a given material should be improved by enhancing the surface area-to-volume ratio. This can be achieved either by fabricating thin film devices or by using nano-scaled materials [12 (and references therein)–14], such as fine-grained precursor powders.

In the following, a wet-chemical synthesis method for preparing nano-sized $SrTi_{1-x}Fe_xO_{3-\delta}$ powders is described. The sensor performance of thick films prepared from these precursors is evaluated. The functionality of the nano-sized particles is compared to micro-scaled powders obtained by a conventional solid-state reaction and to thin film devices.

2. Experimental

Conventional powders of the p-type semiconductors $Sr(Ti_{0.8}Fe_{0.2})O_{3-\delta}$ were prepared from the precursor materials $SrCO_3$ (Technipur, Merck, Germany), TiO_2 (Merck, Germany) and Fe_2O_3 (AlfaAesar, Johnson Matthey GmbH, Germany) following the mixed oxide route. After calcination at 1200 °C, the powders were ball-milled. By laser diffraction (Mastersizer 2000, Malvern Instruments), a particle size of 1.7 μm d_{50} was determined. These rather coarse powders, which serve as base materials for screen-printing pastes and targets for pulsed laser deposition, are referred to as MO powders in the following.

The synthesis of sol-precipitated nano-powders followed a titanate preparation route described by Zheng et al. [15] with a slight modification. As precursors, $Sr(NO_3)_2$, $Fe(NO_3)_3{\cdot}9H_2O$ and titanium isopropoxide (all Fluka) were used in stoichiometric proportions. The precipitation reaction was conducted in continuously stirred aqueous solution. The pH value was adjusted using glacial acetic acid. In contrast to the original method, no 4 M NaOH was added at this point of the synthesis. The solution was heated to 80 °C and kept at this temperature for 3.5 h. Then powder precipitation was initiated by addition of 4 M NaOH. The reaction product, which is denoted as SP powder in the following, is subsequently calcined at 850 °C for 3 h.

In both cases, phase purity of the samples was assured by XRD measurements (Phillips X'Pert-MPD-PW3040/00) with monochromated Cu Kα radiation ($10° \leq 2\Theta \leq 90°$). Invariably, all peaks of the obtained XRD spectra could be indexed assuming a pseudo-cubic perovskite lattice.

The interdiffusion of elemental components of $Sr(Ti_{1-x}Fe_x)O_{3-\delta}$ thick films and alumina substrates is a known problem that can be eliminated by applying a $SrAl_2O_4$ underlayer between the alumina substrate and the electrodes as described elsewhere [16]. According to former results [10], the use of platinum for electrical contacting is very advantageous. Hence, either a set of four platinum electrodes or two platinum interdigitated electrodes (IDE) were applied onto the substrate prior to $Sr(Ti_{1-x}Fe_x)O_{3-\delta}$ film deposition. After sintering at 1100 °C (MO powders) or 850 °C (SP powders) in air for 1 h, the film thickness was determined by a profilometer to be between 10 and 20 μm. The sensor configuration is shown in Fig. 1.

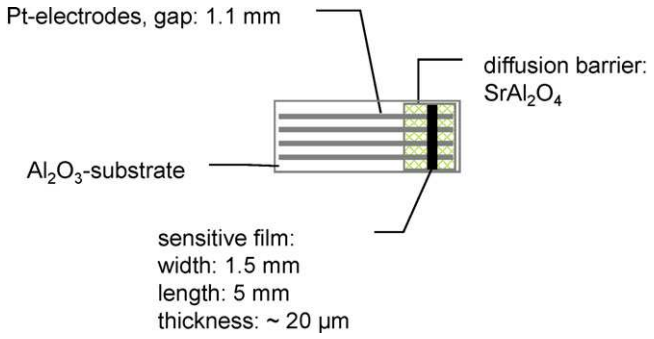

Fig. 1. Diagrammatical presentation of the thick film sensor devices including the dimensions of the active thick film sensor layer. As an alternative, interdigitated Pt electrodes (100 μm line and spacing) were used.

For the pulsed laser deposition (PLD) of thin films, a pressed pellet was prepared from the MO powders and densely sintered at 1520 °C. This as-prepared target was used to deposit thin films on substrates of polycrystalline alumina equipped with a strontium aluminate film and platinum IDEs. An excimer laser (KrF Lambda Physik, LPX305*i*) with wavelength $\lambda = 248$ nm, at a pulse frequency of 8 Hz, and energy of 600 mJ was used to deposit the films. The energy fluence at the target was estimated to be ~1.6 J/cm^2. Depositions were carried out under an oxygen atmosphere at a partial pressure of 13 Pa, with a heated substrate held isothermally at 700 °C. After annealing at the same temperature for 30 min under an oxygen partial pressure of 53 kPa the films were cooled to room temperature at 10 °C/min. The thickness of the films was estimated to be 200 nm from previous calibrations.

For determining sensor functionality, the specimens were either heated to the corresponding operating temperature in a tube furnace, or they were mounted directly in a sample chamber and heated via a platinum thick-film heater structure on the sensor backside. In the entire study, the temperature range from 350 to 500 °C was covered. In the present paper, sensor tests focused on measurements at 400 °C.

Using mass flow controllers, different analyte gases were added to a reference nitrogen flow containing 20 vol% of oxygen. Total gas flow was adjusted either to 600 ml/min for the sensors in the tube furnace or to 6 l/min in the case of the actively heated sensors. Before each measurement, samples were heated at 400 °C for several hours to allow for thermal equilibration. Before adding analytes gases, the furnace or the sample chamber was purged with the reference composition of 20% oxygen in nitrogen for at least 20 min until a stable baseline was observed.

Hydrocarbon (HC) sensitivity was measured for propane (300–2500 ppm) and propene (80–1000 ppm). In order to compare the effect of hydrocarbons with different reactivity or a different chain length, sensor response towards methane, propane, propene and butane was also investigated. To assure comparability, the concentration of these different hydrocarbon species C_nH_m was chosen so that total concentration of carbon atoms $c_{TCA} = n^{\bullet} c_{C_nH_m}$ was kept constant at 1500 ppm. Hence, $c_{\text{methane}} = 1500$ ppm, $c_{\text{propane}} = c_{\text{propene}} = 500$ ppm and $c_{\text{butane}} = 375$ ppm. In addition, a mixture of hydrocarbons

(HC mix, 375 ppm) containing ethane, ethene, acetylene and propene in equal proportions was tested.

In order to study response to interference gases, similar measurements were conducted with CO, NO (both 500–750–1000 ppm) and H_2 (5000–2500–1000 ppm). In addition to the actual values of the mass flow controllers, the gas composition was verified analytically using an FTIR spectrometer (except for H_2). The dc-sensor resistance of all sensor devices was monitored with a Keithley 2700 digital multimeter.

3. Results and discussion

Fig. 2a and b presents SEM micrographs (Leo 1450 VP) of thick films prepared from different base powders, both taken at the same magnification. The MO powders (Fig. 2a) obtained via a solid-state reaction are very porous and coarse-grained with grain sizes of up to 1.2 μm after film sintering. By the wet-chemical route, however, very fine powders are obtained. The grain diameters are about 70 nm (Fig. 2b). At a lower magnification (Fig. 2c), however, one notes a coagulation of the fine particles into larger agglomerates. These coarse secondary particles are observed only after calcinations. Such a formation of agglomerates is often observed for nano-powders and an important problem in nano-sintering [17]. In the case of porous thick films, however, there is no need to avoid the coagulation process since the surface of the single particles is still accessible to gas exposure.

Additional multi-point BET measurements (Micromeritics ASAP 2010, adsorptive: N_2) conducted on the powders yielded specific surface areas of 3 m^2/g for conventional MO powders and up to 20 m^2/g for SP powders, thus indicating a smaller grain size of the SP particles. These findings are in agreement with the SEM results.

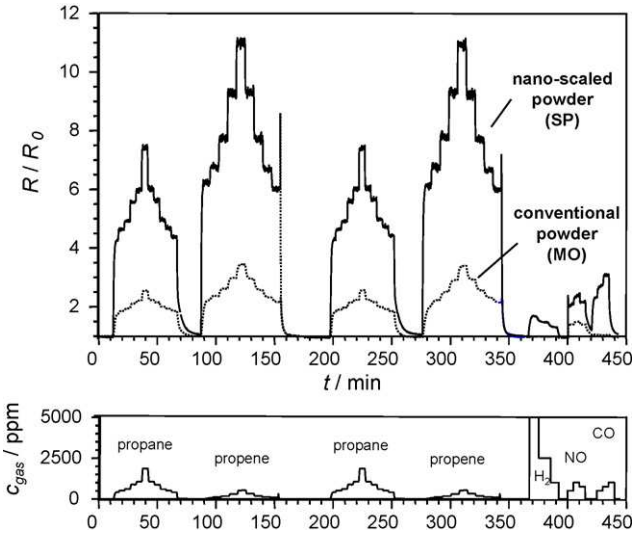

Fig. 3. Comparison of the normalized sensor signals of a conventional (dashed line) and of a nano-scaled SP-based (solid line) $Sr(Ti_{0.8}Fe_{0.2})O_{3-\delta}$ sensor at 400 °C in dry air (upper part). Analyte gas concentrations as indicated (lower part).

Typical conductometric response curves of a conventional MO-based sensor device (dashed line) and a thick film sensor prepared from sol-precipitated powder (solid line) are shown in Fig. 3. For comparing the sensor characteristics of the sensor films, the resulting resistance change response R/R_0 (as defined in ref. [18]) are plotted.

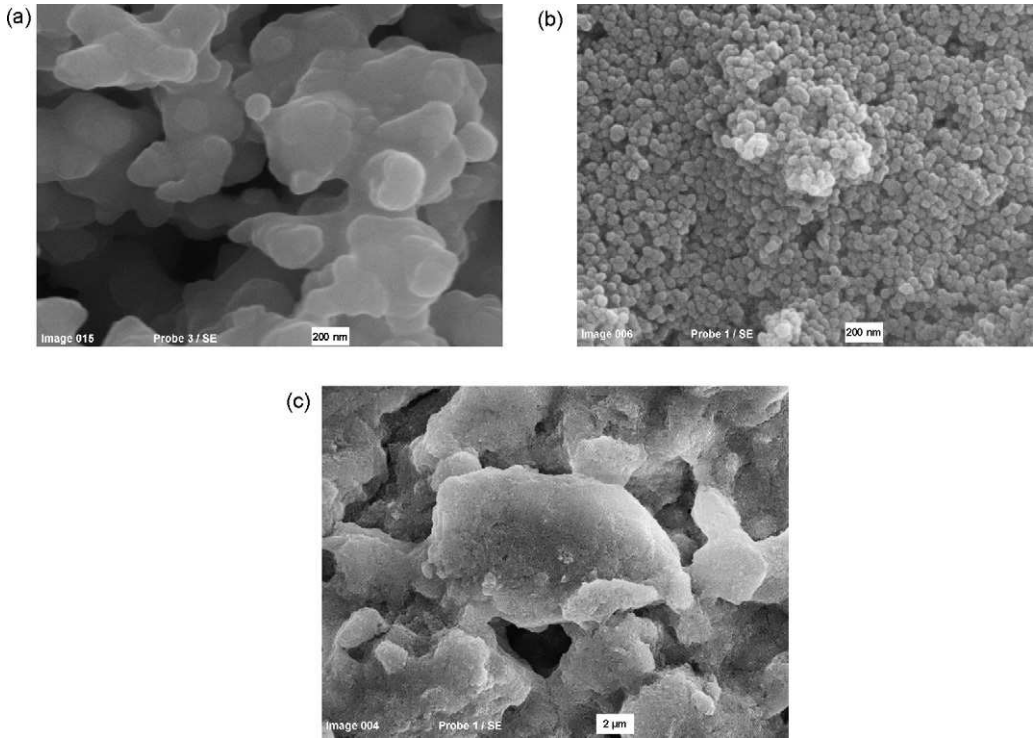

Fig. 2. SEM micrographs of a conventional sensor film (a) and of a fine grained sol-based film (b). In addition, an SEM micrograph of the SP film at lower magnification is given in (c).

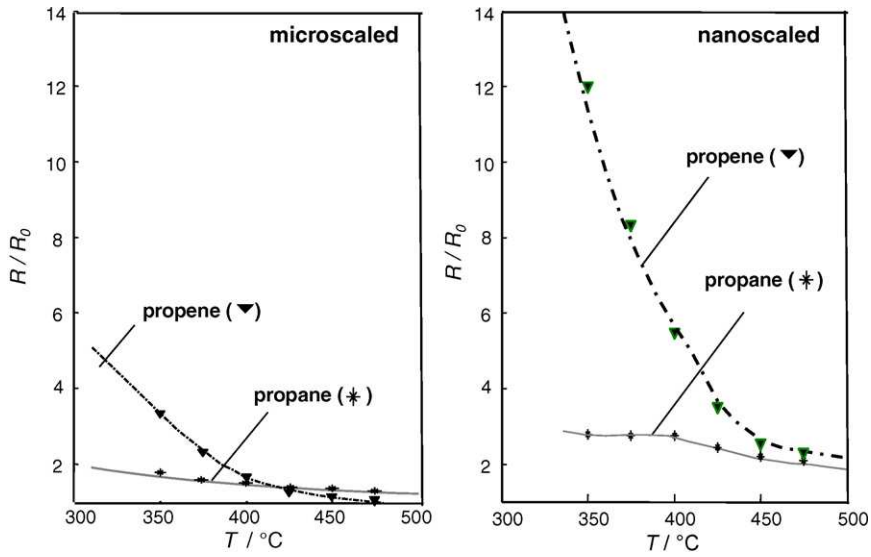

Fig. 4. Comparison of the normalized sensor signals of micro-scaled (left) and nano-scaled SP-based (right) $Sr(Ti_{0.8}Fe_{0.2})O_{3-\delta}$ sensors at different temperatures in dry air. The lines have been inserted as a guide to the eye. Analyte gas concentrations: 500 ppm propane and 500 ppm propene, respectively.

Both sensors show a fast, reversible and reproducible response towards propane and propene, and each has a very stable baseline. The base resistance in air, R_0, of SP powders (in the order of 300–400 kΩ at 400 °C) was found to be higher than that of MO powders (in the order of 1–3 kΩ at 400 °C). This is attributed to the fine-grained microstructure of the SP sensor films, where the firing temperatures are very low, and consequently almost no sintering occurs. Hence, current pathways are passing through many narrow interparticle contacts or "necks", which contribute to total resistivity, and high resistance values are observed.

Whereas the conventional MO powder reaches a maximum change R/R_0 of only 3.5 when exposed to 1000 ppm propene, the nano-scaled SP-based sensor shows a more pronounced response for both hydrocarbons. In this case a maximum R/R_0 value of 11.2 is observed during propene exposure. Minor cross-interference of NO, CO and H_2 is observed, whereas the conventional device only presents a cross-sensitivity towards NO.

Thus, the hydrocarbon sensitivity of an $Sr(Ti_{1-x}Fe_x)O_{3-\delta}$ thick film device is improved by applying nano-scaled SP-based materials. As shown in Fig. 4 for 500 ppm propane and propene, this trend was valid over the temperature range from 350 to 500 °C. Keeping in mind the tradeoff between the slower response at low temperatures and the lower signal at high temperatures (cf. Fig. 4), the following sections focus on measurements at 400 °C, which had been identified previously as the optimum operating temperature [9].

A mechanistic model describing this phenomenon, which is attributed essentially to the enhanced surface-to-volume ratio, has been proposed elsewhere [19,20]. A method to reduce the cross-sensitivities by means of a zeolite layer as reported in ref. [11] is discussed below.

Sensitivity m, which describes the ratio of the change in sensor output to the change in the value of the measurand, was also determined using the following power law:

$$R \propto c_{HC}^{m} \quad (1)$$

where c_{HC} is the hydrocarbon concentration and R is the sensor resistance.

To determine the value of m, sensor response measurements were conducted in the range from 100 to 2000 ppm (propane) and 80 to 1000 ppm (propene). Fig. 5 shows a double-logarithmic representation of the results of the sensitivity tests for propane and propene, where $\log R = f(\log c_{HC})$. This analysis yields a linear relationship with the slope m, which is commonly used as a measure of sensitivity. For both hydrocarbon species, the use of a fine-grained precursor powder leads to a notable increase in sensor sensitivity. In the case of propane, m increases from 0.22 to 0.4, whereas propene sensitivity changes from $m = 0.25$ to 0.38. This is in agreement with findings reported for other semiconducting sensor materials, where a decrease in size leads to enhanced sensitivity [14,21]. As the sensing behavior of perovskite semiconductor sensors is attributed to a redox reaction taking place at the sensor surface, the enhanced surface/volume ratio increases the role of surface states in the sensor response.

In Fig. 6, typical relative resistance R/R_0 values of $Sr(Ti_{0.8}Fe_{0.2})O_{3-\delta}$ sensors are presented for a variety of hydrocarbons. Thick films prepared from MO and SP powders are compared to PLD thin films.

According to these results, the performance of sol-precipitated powders ranges between conventional MO thick films and thin film sensors for unsaturated hydrocarbons and long HC chains. For short saturated HC species such as methane or propane, where the sensitivity of thin films is reported to be low [10], the SP device performs best. Integration of PLD thin films and SP based thick films on a single sensor chip could thus lead to a very sensitive hydrocarbon sensor, which in addition has the potential to discriminate between saturated and unsaturated hydrocarbons.

In Table 1, t_{90} values, i.e., the time at which the sensor output reaches 90% of its final value, are summarized for the different $Sr(Ti_{0.8}Fe_{0.2})O_{3-\delta}$ sensors at 400 °C in response to a step change in concentration of 500 ppm of propane and propene.

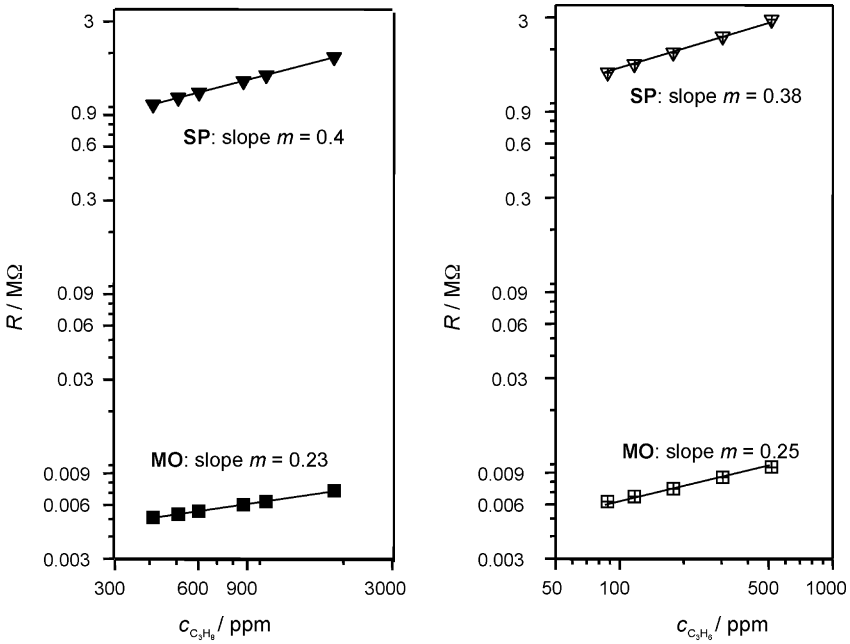

Fig. 5. Propane (left) and propene (right) sensitivity of $Sr(Ti_{0.8}Fe_{0.2})O_{3-\delta}$ sensor films based on MO and SP precursor powders at 400 °C.

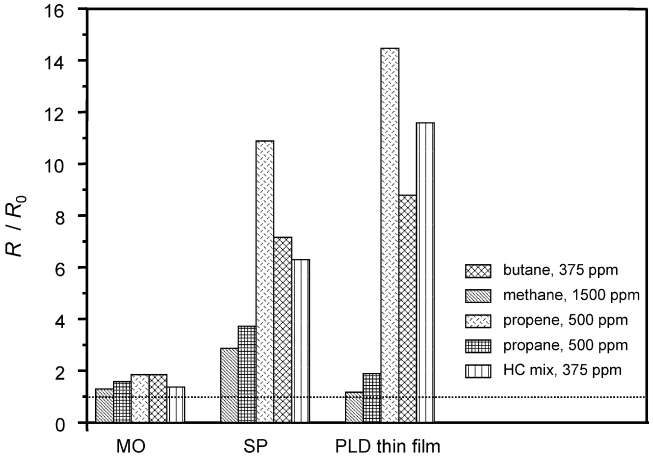

Fig. 6. Relative resistance R/R_0 of $Sr(Ti_{0.8}Fe_{0.2})O_{3-\delta}$ sensor films at 400 °C. Gases and concentrations as indicated in dry air. R_0 values: 1.46 kΩ (MO powder), 349 kΩ (SP powder) and 1320 kΩ (PLD, thin film).

The response times of SP based thick films are comparable to those for the MO powders and are faster than the responses found for PLD thin films. Thus, the nano-scaled thick film devices combine the fast sensor response of $Sr(Ti_{0.8}Fe_{0.2})O_{3-\delta}$ thick films with the high R/R_0 values observed for thin films.

Table 1
Response times t_{90} of different $Sr(Ti_{0.8}Fe_{0.2})O_{3-\delta}$ sensor films at 400 °C towards 500 ppm propane and propene

	t_{90} (s)		
	MO thick film	SP thick film	PLD thin film
Propane, 500 ppm	85	150	>975[a]
Propene, 500 ppm	155	130	255

[a] After 20 min, the thin film had not reached a stable plateau value. The presented t_{90} value has been calculated using the final reading before propane injection was stopped.

By covering a nano-scaled $Sr(Ti_{0.8}Fe_{0.2})O_{3-\delta}$ film with a 50 μm thick Pt-doped ZSM5 (1.6 wt% of Pt, cation ratio $Na^+/H^+ = 85:15$) layer, one obtains a very sensitive and selective hydrocarbon sensor as shown in Fig. 7. Compared to a conventional MO thick film sensor (dashed line), the sensor performance is considerably improved with respect to both sensitivity and selectivity. By applying the zeolite layer, the cross-interference of NO and CO has been effectively eliminated. This is because the ZSM5 zeolite is an excellent oxidation catalyst, and while passing through the zeolite layer, CO is oxidized to CO_2 prior to reaching the sensor layer [11]. In the case

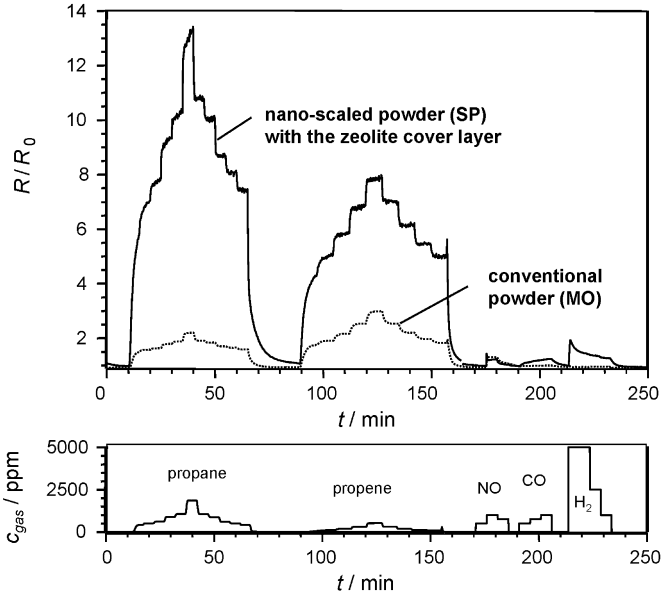

Fig. 7. Relative resistance R/R_0 of a zeolite-covered $Sr(Ti_{0.8}Fe_{0.2})O_{3-\delta}$ SP film and a MO film at 400 °C. Gases as indicated in dry air. R_0 values: 2.80 kΩ (MO powder) and 277 kΩ (SP powder).

of NO, one part of the interfering gas is converted to NO_2 according to the corresponding NO–NO_2 equilibrium. This conversion was verified with additional catalytic tests on the zeolite powder. In both cases, response of the $Sr(Ti_{0.8}Fe_{0.2})O_{3-\delta}$ film is suppressed because the analyte species does not reach the sensor layer. Noteworthy is the increase of propane sensitivity that is observed when the zeolite layer is present. This observation is currently being investigated and possibly due perhaps to partial oxidation of propane to some other active compound.

In an additional measurement series, the impact of humidity on propane sensitivity of sensors with and without the zeolite layer was investigated. For this purpose, 2.5 vol% of water vapor was added to the reference gas flow. The presence of humidity was found to suppress the propane sensitivity of the bare sensor films to some extend. At 500 ppm, for example, the sensor signal decreased from 1.6 to 1.3, no cross-interference was observed for the zeolite covered layers (for details see ref. [19], additional results will be discussed in a forthcoming paper). This was attributed to the fact that water vapor tends to adsorb in the zeolite channels, so that it does not reach the sensor surface. The zeolite layer thus enables the effective reduction of various cross-interfering species.

4. Conclusion

Sol-derived nano-scaled $Sr(Ti_{0.8}Fe_{0.2})O_{3-\delta}$ powders can be used as precursors for screen-printed p-type conductometric hydrocarbon sensors. Such devices show a fast and sensitive response, and the signal is found to be stable and reproducible. In addition, they perform better than conventional micro-scaled thick films over the entire temperature range from 350 to 500 °C. The size of the precursor powders for $Sr(Ti_{1-x}Fe_x)O_{3-\delta}$ sensors is a crucial parameter in order to improve sensor functional qualities. Further investigation will therefore be directed to other synthesis methods for nano-materials, such as electrospraying or electrospinning, in order to confirm these promising results.

As another approach for selectivity enhancement, the use of PLD thin films, which present a good selectivity towards unsaturated hydrocarbons such as propene, was tested successfully. Finally, the use of a catalytically active zeolite cover layer provided a further selectivity enhancement by effectively reducing the cross-interference of NO and water vapor.

Acknowledgements

The authors thank Ms. Monika Wickles for sample preparation, Mr. Hans-Jürgen Deerberg for SEM micrographs, Mrs. Ingrid Otto and Mr. Hannes Wolf for BET measurements and Dr. Andreas Dubbe and Mr. Gunter Hagen (all University of Bayreuth) for zeolite preparation.

Financial support of this project was provided through a joint international program of the National Research Council of Canada, the Helmholtz Gemeinschaft and German Federal Ministry of Education and Research (BMBF) and is gratefully acknowledged (Projects NRCC-21-CRP-02 and 01SF0201 9.2).

References

[1] N. Docquier, S. Candel, Combustion control and sensors, a review, Prog. Energy Combust. Sci. 28 (2002) 107–150.
[2] B. Timmer, W. Olthuis, A. van den Berg, Ammonia sensors and their applications—a review, Sens. Actuators B 107 (2005) 666–677.
[3] J. Riegel, H. Neumann, H. Wiedenmann, Exhaust gas sensors for automotive emission control, Solid State Ionics 152–153 (2002) 783–800.
[4] R. Moos, A brief overview on automotive exhaust gas sensors based on electroceramics, Int. J. Appl. Ceram. Technol. 2 (2005) 401–413.
[5] T. Moser, F. Stanglmeier, B. Schumann, S. Thiemann-Handler, Sensor in planarer Dickschichttechnik zur Messung von Kohlenwasserstoffen im Abgas von Kraftfahrzeugen (Planar thick-film sensor for measuring hydrocarbons in automotive exhausts), in: VDI-Berichte 1530, VDI-Verlag, Ludwigsburg, Germany, 2000, pp. 159–167.
[6] D. Niemeyer, D.E. Williams, P. Smith, K.F. Pratt, B. Slater, C.R.A. Catlow, A.M. Stoneham, Experimental and computational study of the gas-sensor behaviour and surface chemistry of the solid-solution $Cr_{2-x}Ti_xO_3$ ($x < 0.5$), J. Mater. Chem. 12 (2002) 666–675.
[7] Y. Li, W. Wlodarski, K. Galatsis, S.H. Moslih, J. Cole, S. Russo, N. Rockelmann, Gas sensing properties of p-type semiconducting Cr-doped TiO_2 thin films, Sens. Actuators B 83 (2002) 160–163.
[8] G. Martinelli, M.C. Carotta, M. Ferroni, Y. Sadaoka, E. Traversa, Screen-printed perovskite-type thick film gas sensors for environmental monitoring, Sens. Actuators B 55 (1999) 99–110.
[9] K. Sahner, R. Moos, M. Matam, J. Tunney, M. Post, Hydrocarbon sensing with thick and thin film p-type conducting perovskite materials, Sens. Actuators B 108 (2005) 102–112.
[10] K. Sahner, R. Moos, M. Matam, M. Post, Effect of electrodes and zeolite cover layer on hydrocarbon sensing with p-type perovskite $SrTi_{0.8}Fe_{0.2}O_{3-\delta}$ thick and thin films, J. Mater. Sci. 41 (2006) 5828–5835.
[11] K. Sahner, R. Moos, M. Matam, M. Post, Use of a zeolite cover layer for improving sensor characteristics of p-type conducting perovskites, in: Sensor 2005 Proceedings, vol. I, Nuermberg, Germany, May 2005, pp. 201–206.
[12] P.I. Gouma, Nanostructured polymorphic oxides for advanced chemosensors, Rev. Adv. Mater. Sci. 5 (2003) 147–154.
[13] V. Guidi, M.C. Carotta, M. Ferroni, G. Martinelli, L. Paglialonga, E. Comini, G. Sberveglieri, Preparation of nanosized titania thick and thin films as gas-sensors, Sens. Actuators B 57 (1999) 197–200.
[14] E. Comini, G. Faglia, G. Sberveglieri, D. Calestani, L. Zanotti, M. Zha, Tin oxide nanobelts electrical and sensing properties, Sens. Actuators B 111–112 (2005) 2–6.
[15] H. Zheng, X.Q. Liu, G.G. Meng, O.T. Sorensen, Fine $SrTiO_3$ and $Sr(Mg_{0.4}Ti_{0.6})O_{3-\delta}$ perovskite ceramic powders prepared by a sol-precipitation process, J. Mater. Sci.: Mater. Electron. 12 (2001) 629–635.
[16] R. Moos, F. Rettig, A. Hürland, C. Plog, Temperature-independent resistive oxygen exhaust gas sensors for lean-burn engines in thick-film technology, Sens. Actuators B 93 (2003) 43–50.
[17] J.R. Groza, Nanosintering, Nanostruct. Mater. 12 (1999) 987–992.
[18] A. D'Amico, C. Di Natale, A contribution on some basic definitions of sensor properties, IEEE Sens. J. 1 (2001).
[19] K. Sahner, Modeling of p-Type Semiconducting Perovskites for Gas Sensor Applications, Shaker Verlag Aachen, Germany, 2006, ISBN 3-8322-5538-9.
[20] K. Sahner, R. Moos, Modeling of hydrocarbon sensors based on p-type semiconducting perovskites, Phys. Chem. Chem. Phys. 9 (2007) 635–642.
[21] G. Bläser, Th. Rühl, C. Diehl, M. Ulrich, D. Kohl, Nanostructured semiconductor gas sensors to overcome sensitivity limitations due to percolation effects, Phys. A: Stat. Theor. Phys. 266 (1999) 218–223.

Biographies

Kathy Sahner received her German engineering diploma in materials science from the Saarland University, Germany, in 2002. At the same time, she also received the corresponding French degree from the European School of Materials Science and Engineering (EEIGM), France. During her PhD, she investigated

of gas sensitive perovskites including mechanistic modeling. She then worked as a postdoctoral researcher at the University of Bayreuth, Germany, and at the Massachusetts Institute of Technology, USA, on various projects within the field of electroceramics. Her current research interests focus on materials for gas sensor applications, transport phenomena in sensor films, and ion conductors.

Daniela Schönauer received her engineering diploma in materials science in 2005 from University of Bayreuth, Germany. Since 2006, she is a PhD student at the chair of Functional Materials at the University of Bayreuth. Her research interests are gas sensor applications and exhaust gas aftertreatment systems.

Mahesh Matam after obtaining his PhD from India in ferroelectrics/piezoelectric ceramics, worked at Simon Fraser University (SFU), Vancouver as a post doctoral fellow. At SFU he grew single crystals and thin films of piezoelectric materials before moving to the National Research Council of Canada (NRCC) in Ottawa as a Visiting Fellow. His focus at NRCC was on growing and characterizing thin perovksite oxide films for hydrocarbon sensing using pulsed laser ablation. In 2006, he moved into the piezo-ceramics industry where he currently works on R&D projects related to ultrasonic sensors. He works for Piezotechnologies in Indianapolis, Indiana and can be reached at mmatam@piezotechnologies.com.

Michael Post received his PhD in chemistry from the University of Surrey, UK, in 1971 and is a Principal Research Officer and leader of the sensor and devices project at the ICPET institute of the National Research Council of Canada, where he has been an active researcher in materials science since 1975. Projects have included X-ray diffraction and structure determination, intermetallic compounds for hydrogen storage and phase studies of high temperature superconducting ceramics. Recent research interests are directed toward the investigation of structural and functional relationships of thin and thick film non-stoichiometric compounds and nanomaterial composites for application as gas sensors.

Ralf Moos received his diploma in electrical engineering in 1989 from University of Karlsruhe, Germany. As a PhD student, he conducted research on defect chemistry of titanates. In 1995, he joined DaimlerChrysler and worked in the serial development of exhaust gas aftertreatment systems. In 1997, he moved to DaimlerChrysler Research in Friedrichshafen, where he headed several projects in the field of exhaust gas sensing. Since 2001, he is head of the Chair of Functional Materials of the University of Bayreuth. His main research interest are materials and systems for exhaust gas aftertreatment, gas sensing, and gas sensor technology.